Biochimica et Biophysica Acta, 987 (1989) 154–164
Elsevier

BBAMEM 74662

Membrane electrogenesis in plasmodia of *Physarum polycephalum*: a dominant role for the proton pump

H. Kuroda [1], R. Kuroda [1] and T. Sakai [2]

[1] *Sugashima Marine Biological Laboratory, School of Science, Nagoya University, Toba and* [2] *Research and Development Division, Yoshitomi Pharmaceutical Industries, Ltd., Osaka (Japan)*

(Received 22 June 1989)

Key words: Electrogenic proton pump; Membrane potential; ATP; Proton efflux; (*P. polycephalum*)

An electrogenic ion pump, previously identified in caffeine-induced plasmodial droplets of *Physarum*, is here shown to be the major source of the resting membrane potential of intact *Physarum* plasmodia, and to be an H^+-ATPase. The plasma membrane of plasmodia is rapidly depolarized by the respiratory inhibitors, cyanide and azide, which cause an almost parallel depletion of intracellular ATP. It is also depolarized by the ATPase inhibitors, diethylstilbestrol and orthovanadate. Diethylstilbestrol, however, produces only a slight depletion of ATP. Plots of membrane potential versus intracellular ATP concentration, during the onset of cyanide inhibition, yield a saturation curve which can be fitted by the Michaelis equation (describing the pump) plus a constant term (describing ion diffusion), with maximal voltage of the pump $\cong -120$ mV, $K_m \cong 1.1$ mM, and the diffusion term $= -4$ mV. Intracellularly injected ATP hyperpolarizes plasmodial membranes to the expected level. Direct measurements of proton flux show net efflux of 14 pmol $\cdot s^{-1} \cdot mg^{-1}$ (dry weight) in uninhibited plasmodia, which converts to 28 pmol $\cdot s^{-1} \cdot mg^{-1}$ net influx during 80 s of cyanide inhibition. This efflux minimum coincides in time with the membrane potential minimum. Bidirectionality of net proton flux suggests a significant role of H^+ for passive diffusion.

Introduction

This report constitutes the second half of a two-part study on ionic mechanisms in cell membranes of the slime mold *Physarum polycephalum*. In the first part [1], we described the operation of an electrogenic ion pump in the surface membrane of cytoplasmic droplets formed by briefly incubating *Physarum* plasmodia in 5–10 mM caffeine solutions. Indirect evidence indicated that the pumped ion current in droplet membranes must be hydrogen ions, as had also been found in true fungi such as *Neurospora* [2,3] and *Saccharomyces* [4], in charophyte algae such as *Nitella* [5,6], *Chara* [7] and *Nitellopsis* [8], and in several tissues of higher plants, including red beet storage tissue [9,10]. Also by comparison with the experiments on fungi, algae, and higher plants, the electrogenic pump in plasmodial droplets was expected to be an ATPase, but neither ATP consumption nor H^+-extrusion during pump operation was directly demonstrated.

The central purpose of the present experiments, then, has been to describe the relationships among intracellular ATP concentration ($[ATP]_i$), net proton flux, and the difference of electric potential across *Physarum* membranes, in order to determine whether the pump is, in fact, an H^+-ATPase. An important secondary purpose has been to determine the relative contributions of ion pumping and ion diffusion to the total membrane potential. In the first part [1], we employed the caffeine-induced cytoplasmic droplets as the experimental material, because at that time they had tolerated intracellular electrodes for much longer periods than intact plasmodia. However, recent technical improvements in the experiments, especially in construction of microelectrodes, permit long-term recording from intact plasmodia of *Physarum polycephalum*. Additionally, droplets have disadvantages for preparation of a large quantity of homogeneous materials, which is prerequisite for ATP and proton flux measurements. Now, we have adopted a more physiological and conventional

Abbreviations: DES, diethylstilbestrol; EGTA, ethyleneglycol-bis(β-aminoethyl ether)-*N,N,N',N'*-tetraacetic acid; Pipes, 1,4-piperazinediethanesulfonic acid; Hepes, 4-(2-hydroxyethyl)-1-piperazineethanesulfonic acid; Mes, 4-morpholineethanesulfonic acid; Pa, phthalic acid; Dmg, 3,3-dimethylglutaric acid.

Correspondence: H. Kuroda, Sugashima Marine Biological Laboratory, School of Science, Nagoya University, Sugashima-cho, Toba-shi, Mie-ken 517, Japan.

preparation, in preference to the cytoplasmic droplets. Both normal plasmodia cultivated on wet oatmeal and microplasmodia (200–500 μm diameter) grown in liquid media have been examined. Variations of ion pumping, and concomitant changes, have been followed at the onset and/or release of inhibition both by general metabolic inhibitors (potassium cyanide and sodium azide) and by direct pump inhibitors (diethylstilbestrol (DES) and sodium orthovanadate), and the ATP-dependence of pumping has been quantified by direct intracellular injections of ATP.

Materials and Methods

Plasmodia

Physarum polycephalum was grown in two types of cultures. First, according to the method of Daniel and Rusch [11], plasmodia were cultivated as shaking cultures in a semi-defined sterile liquid medium (see below), dark, with a shaker drawing 8-shaped locus, at approx. 100 rpm and 19–20 °C. These conditions optimize formation of microplasmodia, which were harvested by centrifugation ($200 \times g$ for 2 min at 19–20 °C) during log-phase proliferation, washed, and resuspended in standard 1,4-piperazinediethanesulfonic acid (Pipes) buffer (see Table I). The resulting microplasmodial suspensions were incubated as standing cultures, bubbled with 100% O_2 at 20 °C, for a few hours until use. For normal giant plasmodia, the organism was cultivated according to the method of Camp [12], as stationary cultures on wet oatmeal, dark, at 18–20 °C. Two or three days before the experiments, small plasmodial masses were transferred to agar plates (3 g/dl agar in distilled water) containing no added salts or nutrients.

Media

Cultivation medium for microplasmodia, modified slightly from that of Daniel and Rusch [11], contained the following: 10 mg/ml trypton (Difco Corp., Detroit, MI, U.S.A.), 1.5 mg/ml yeast extract (Difco), 10 mg/ml glucose, 50 μg/ml hemin, 1 mM $CaCl_2$, 1 mM $MgSO_4$, 0.2 mM $FeSO_4$, 0.1 mM $MnCl_2$, 0.03 mM $ZnSO_4$, 15 mM KH_2PO_4, and 10 mM sodium citrate, (a final pH of 4.5). Ten additional solutions were used, for which the explicit compositions are shown in Table I. These include standard Pipes buffer for electrical recordings and ATP measurements, dilute Pipes buffer for pH recordings, four test pH media, and four test K^+ media. Finally, all inhibitors and nucleotides to be used for intracellular injections were dissolved in a solution of 10 mM ethyleneglycol-bis(β-aminoethyl ether)-*N,N,N',N'*-tetraacetic acid (EGTA) plus 10 mM Pipes-KOH (pH 7.0). Inhibitors used were KCN and NaN_3 (Yoneyama Chemical Company, Tokyo, Japan), DES (Tokyo Kasei Industry, Tokyo, Japan) and sodium orthovanadate (Sigma Chemical Co., St. Louis, MO, U.S.A.), and the nucleotides were ATP and ADP (PL Biochemicals Inc., Milwaukee, WI, U.S.A.) and GTP (Sigma).

Electrical recordings

Individual microplasmodia were transferred from the standing culture (see above) to the recording chamber by means of a large, fluid-filled suction pipette. The recording chamber, mounted on the stage of a compound microscope, consisted of a flat rectangular opening cut into a Lucite plate, with a thin layer of agar spread on the bottom and a glass coverslip fitted on top. Perfusion fluids entered through a channel bored near the chamber bottom, and exited through a channel

TABLE I

Composition of experimental media

Name	Concentration (mM)								pH
	K^+	Na^+	Ca^{2+}	Cl^-	$CH_3SO_3^-$	buffer		Glucose	
Standard Pipes	11.4	0	1.0	2.0	0	Pipes	6.7	55.6	6.8
Dilute Pipes	11.4	0	1.0	2.0	0	Pipes	1.0	55.6	6.8
pH 6.0-	11.4	0	1.0	2.0	0	Mes [a]	50.0	55.6	6.0
pH 5.5-	11.4	0	1.0	2.0	0	Mes	20.0	55.6	5.5
pH 4.7-	11.4	0	1.0	2.0	0	Pa [b]	6.7	55.6	4.7
pH 3.7-	11.4	0	1.0	2.0	0	Dmg [c]	20.0	55.6	3.7
1.0 K-	1.0	11.4	1.0	2.0	1.0	Pipes	6.7	55.6	6.8
3.0 K-	3.0	11.4	1.0	2.0	3.0	Pipes	6.7	55.6	6.8
10.0 K-	10.0	11.4	1.0	2.0	10.0	Pipes	6.7	55.6	6.8
30.0 K-	30.0	11.4	1.0	2.0	30.0	Pipes	6.7	55.6	6.8

[a] Mes, 4-morpholineethanesulfonic acid.
[b] Pa, phthalic acid.
[c] Dmg, 3,3-dimethylglutaric acid.

diagonally across the chamber at the top. The total chamber volume was approx. 2 ml, and the flow rate, 3–5 ml/min. All media were prebubbled with 100% O_2 and warmed to 23°C. Microelectrodes were inserted through tapered slots in the lateral chamber walls.

The microelectrodes were made from 1-mm borosilicate tubing with a central glass fiber on a standard horizontal puller (Model PD-5, Narishige Corp., Tokyo, Japan). They were filled with a solution of 1 M KCl, plus 0.9 M EGTA and 0.1 M EDTA, which was adjusted to pH 8.4–8.5 with aq. KOH. *Physarum* plasmodia quickly sealed off the inserted electrode by surrounding the tip and outer wall with newly formed membrane. In the previous study [1], the electrodes for intact plasmodia were filled with 3 M KCl containing 0.1 M EDTA, which permitted only a few minutes of intracellular recording. Then in order to delay the progress of membrane formation by lowering the local Ca^{2+} concentration around the tip of electrodes, the concentration of Ca^{2+}-chelator in the electrode-filling solution was raised as high as possible, and the concentration of KCl was reduced to 1 M for reasons of solubility. The electrodes used had tip resistances of 20–100 MΩ, and they permitted continuous intracellular recording from microplasmodia for periods of 10–60 min. Other details of the recording system have been described previously [1].

ATP measurements and proton flux

For ATP measurement, approx. 2 g wet-packed microplasmodia were suspended in 25-ml standard Pipes buffer, and bubbled continuously with O_2 at 23°C. ATP was extracted from microplasmodia by two different methods. One is the extraction with hot water. 0.5-ml aliquots were withdrawn at appropriate intervals before and after the addition of inhibitors, poured into 2.5-ml boiling water, and boiled for 15 min [13,14], which were then chilled in ice-water. Supernatant fluids were separated from cell debris by centrifugation (10000 × *g* for 10 min at 0°C) and then quickly frozen in solid carbon dioxide to keep frozen until ATP assay. Cell debris was kept for the determination of protein amounts. The other method is the extraction with cold perchloric acid. Microplasmodial suspension (0.5 ml) was poured into 0.5-ml ice-cold 12% (w/v) perchloric acid, and stood in ice for 2 h with occasional stirring. Acid-insoluble cell debris was removed by centrifugation. Supernatant fluids were neutralized to pH 7.5 with 1 M 4-(2-hydroxyethyl)-1-piperazineethanesulfonic acid (Hepes) and 2 M KOH, and kept frozen until ATP assay. For the calibration, 1 to 100 μM authentic ATP solution was treated in similar ways. ATP was assayed by the modified luciferin-luciferase method [13] using desiccated firefly lanterns (FLE50) (Sigma). Cell debris was dissolved in 1 M NaOH, and the protein amount of each aliquot was determined. $[ATP]_i$ was determined from the ATP amount and the total cell volume of microplasmodia in each aliquot, which was calculated from the protein amount of each aliquot (see below). The two methods of ATP extraction gave essentially identical time-courses for $[ATP]_i$ after the onset of inhibition.

Net proton flux was estimated from the extracellular pH changes of microplasmodial suspensions. About 1.6 g wet-packed microplasmodia were suspended in 20-ml dilute Pipes buffer, and continuously bubbled with O_2 at 23°C. A standard pH minielectrode (Model 39505, Beckman Instruments, Inc., Irvine, CA, U.S.A.) was connected to a Beckman Model 4500 pH meter, and was operated with a precision of 0.001 pH unit. Analog outputs of the pH meter was led to a chart recorder (model MC6601, Watanabe Instruments Corp., Tokyo, Japan). The electrode was calibrated by adding a known amount of acid into the plasmodial suspension, and the dry weight of microplasmodia in the suspension was determined at the end of each experiment. In all cases, observed pH changes of microplasmodial suspension induced by inhibitors were corrected for artificial shifts associated with the inhibitor addition, as controlled by adding in the absence of plasmodia (see Fig. 6B). Thus, net proton flux by 1 mg dry weight microplasmodia was determined.

Other materials and methods

DES obtained from several different commercial sources, needed to be recrystallized before use. An adequate procedure for present purposes was two cycles of dissolution in hot ethanol (70°C) at approx. 0.1 g/ml and crystallization by letting stand at room temperature overnight after the addition of two volumes of hot distilled water (70°C). Purified DES was dissolved in absolute ethanol to be 2 mM stock solution, and 100 μM DES solution was prepared by diluting the stock solution in 20 volumes of standard Pipes buffer or dilute Pipes buffer just before experiments. This solution was applied to plasmodia to attain 5 μM. Thus, the concentration of ethanol was 0.25% in experimental solutions. Ethanol was ascertained to give no effect at this concentration on the plasmodial membrane potential.

Intracellular injection of liquids into the small fragments of plasmodia was carried out by modifying the method of Hiramoto [15]. A small fragment cut off from the advancing margin of plasmodia on an agar plate was used. The injection system consisted of a glass micropipette of 1–3 μm in tip diameter containing the liquid for injection and a small drop of mercury, pressure-tight connecting tubes, and a screw-advancing glass syringe. Injection had to be performed gradually and steadily. In order to check the success of injection, the membrane potential was always monitored with an independent microelectrode located in close vicinity to

the injection site. In those cases when the injected solution became isolated by newly formed membranes, the process was easily recognized by a rapid zeroing of the recorded potential. Such protective behavior is well known in micropipette work with plant and fungal cells [2,16,17]. The volumes of plasmodial fragments ranged from $3 \cdot 10^7$ to $13 \cdot 10^7$ μm^3, and the injection volume was about $1 \cdot 10^5$ μm^3.

Dry weights of microplasmodia were determined after removing the suspension media by centrifugation (300 $\times g$ for 5 min at 20– 25°C) and drying in vacuo for several days. Protein amounts were determined by the method of Lowry et al. [18]. The cell volume of microplasmodia was determined according to the gravimetrical method of Winkler and Wilson [19]. As for microplasmodia used in the present experiments, 1 mg dry weight of microplasmodia corresponded to 2.9 ± 0.4 μl of cell volume (mean $\pm$ 1 S.E., five determinations), 0.40 ± 0.03 (5) mg protein, and 15.2 ± 2.4 (42) mg of wet-packed microplasmodia.

Results

Effects of metabolic inhibitors

In experiments with caffeine-induced plasmodial droplets [1], the clearest evidence for the presence of an electrogenic ion pump was a sharp and reversible depolarization of the membrane, by approx. 70 mV, produced by respiratory inhibitors such as potassium cyanide. This result suggested that similar electrogenic ion pumping in normal plasmodia and microplasmodia would also be revealed by membrane depolarization due to cyanide and other respiratory inhibitors. Furthermore, if this ion pump were an ATPase, as expected from studies on plants and true fungi, drugs known to inhibit plasma membrane ATPases should also depolarize *Physarum* plasmodia. Such drugs include, particularly, DES [20,21] and orthovanadate [21,22].

Typical curves of membrane potential versus time, during blockade by KCN or NaN_3 are shown in Fig. 1. In part A, the microplasmodium began with a resting membrane potential of about -60 mV, and depolarized to about -15 mV within 80 s of superfusion with 10 mM KCN. The initial depolarization was followed after several minutes by spontaneous partial repolarization to about -30 mV before KCN wash-out was begun. When cyanide was washed away, the membrane potential recovered gradually. It did, however, progress beyond the control resting potential for many plasmodia, in this case reaching a level of -80 mV in 4–5 min. Such super recovery is observed also in *Neurospora*, which seems to represent damage repair in cells starting with low membrane potentials (Slayman, C.L., personal communication). 10 mM NaCN had essentially identical effects to those of KCN, indicating that cyanide but not the cation was causal. All major features of this electrical

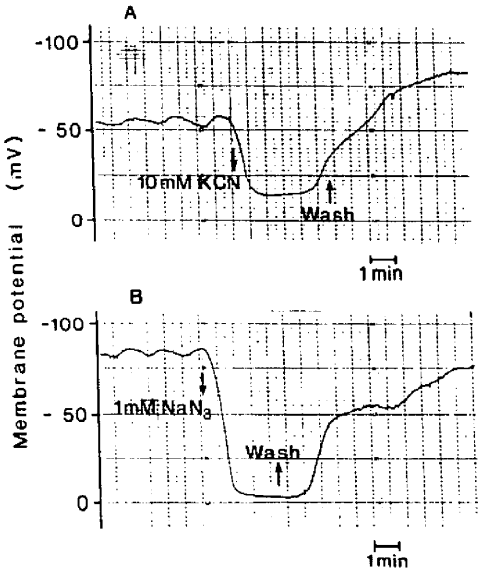

Fig. 1. Depolarization of *Physarum* microplasmodia by KCN (A) and NaN_3 (B). Down arrows: addition of 10 mM KCN or 1 mM NaN_3 to the recording chamber. Up arrows: begin washout of inhibitors. Control recording medium and wash-solution: standard Pipes buffer. Note the start of spontaneous repolarization in the presence of KCN, and hyperpolarization during washout of KCN. Slow oscillations of membrane potential during control recording are characteristic of *Physarum* plasmodia.

response to cyanide were closely similar to those previously found in the caffeine-induced droplets. With intact plasmodia, however, cyanide could be injected directly into plasmodia, and when administered in that fashion, yielded the sudden large depolarization and rapid recovery at approximately 0.01-times the concentration required during extracellular application.

The response of *Physarum* microplasmodia to another respiratory inhibitor, sodium azide (at 1 mM; Fig. 1B) also resembled that to cyanide, although the extent of depolarization was greater, reaching to about -5 mV. The recovery process upon washout of NaN_3 differed more clearly from that with KCN, in showing at least two distinct temporal phases as in *Neurospora crassa* [3]. We have not analyzed the cause of this biphasic behavior, but it may well involve delayed changes of the membrane's passive permeability to ions. Normal plasmodia cultivated on wet oatmeal showed essentially the same responsiveness to cyanide and azide as microplasmodia.

Microplasmodial responses to extracellularly applied ATPase inhibitors were much more variable than the responses to respiratory inhibitors. In some experiments for example, DES, when added to the chamber at a final concentration of 5 μM, had no apparent effect on membrane potential for several minutes (1 to 5 min),

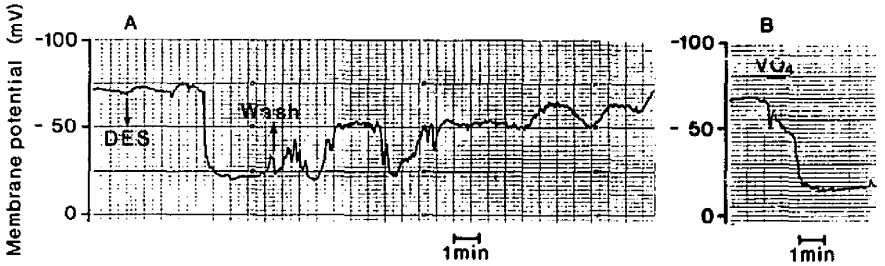

Fig. 2. Depolarization produced by external DES (A) and microinjected orthovanadate (B). (A) Down arrows: addition of 5 μM DES in 0.25% ethanol-standard Pipes buffer. Up arrows: extracellular washout of DES. Record from a microplasmodium. Control medium and wash solution: standard Pipes buffer. Note the abrupt depolarization after approx. 3 min in DES, and the slowly fluctuating recovery during DES washout. (B) Horizontal thick bar: intracellular injection of orthovanadate to approx. 20 μM final concentration into a small fragment of normal plasmodia. The brief transient depolarization at the onset of vanadate injection is an artifact due to penetration of the injection pipette.

and then (after 3 min, in Fig. 2A) elicited rather abrupt depolarization (to about −20 mV, in Fig. 2A). Washout of DES also had irregular effects, usually resulting in slow oscillatory progress toward the control membrane potential, as displayed in Fig. 2A.

Extracellular orthovanadate (20 μM) rarely had any effect on intact microplasmodia. This finding was consistent with observations on *Neurospora*, which led to the discovery that orthovanadate enters via a high-affinity phosphate transport system which is scarce in the plasma membranes of phosphate-replete cells [22], and whose synthesis must be derepressed by prior phosphate starvation [23,24]. Phosphate depletion of *Physarum* was therefore attempted by incubating plasmodia in standard Pipes buffer (phosphate-free) for 10–30 h. Although this usually resulted in some depolarization of the plasmodial membrane by extracellular orthovanadate, the effect was small and erratic, and we turned to the more controllable technique of directly injecting orthovanadate [25], with results as shown in Fig. 2B. As expected, the plasma membrane depolarized sharply, to a steady level of about −15 mV.

Altered $[ATP]_i$ with different inhibitors

An important internal check on the assumptions made above, that cyanide and azide depolarize the plasma membrane through their general metabolic effect by withdrawing substrate ATP, but that orthovanadate and DES inhibit by direct actions on a membrane-bound transport system, would be to determine the correlated effects of the different inhibitors upon metabolism. We have therefore explicitly measured the time-courses of changes in $[ATP]_i$ following treatment of microplasmodia with cyanide (Fig. 3A), and with DES (Fig. 3B). In both plots of Fig. 3, the solid circles show ATP concentrations in microplasmodia for several minutes after addition of the inhibitor, and averaged over three independent experiments. The open circles denote averaged membrane potentials for 9–11 experiments.

It is obvious that with cyanide, $[ATP]_i$ dropped quickly, falling to about 30% of the control level within 70 to 80 s, and that its time-course almost paralleled that for the decline of membrane potential. After the

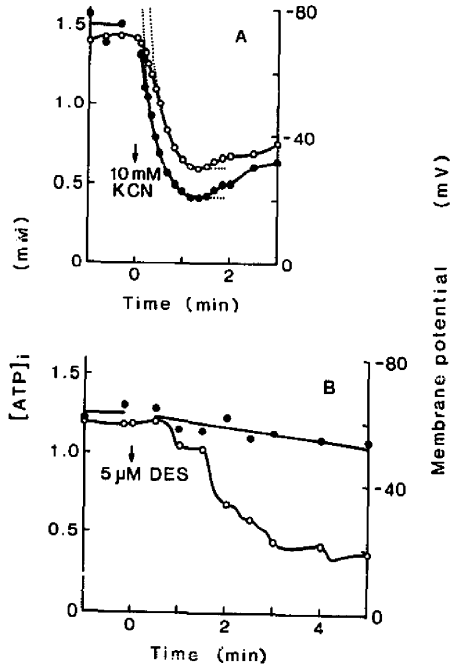

Fig. 3. Comparison of ATP changes with voltage changes in *Physarum*, during inhibition by cyanide (A) or DES (B). 10 mM KCN or 5 μM DES added at zero time in both experiments. Control solution: standard Pipes buffer. $[ATP]_i$ (●) determined at the times plotted; membrane potentials (○) recorded continuously, and values read out at times corresponding to the ATP-sample times. $[ATP]_i$ values are averages for three separate experiments; membrane potential are averages for 9–11 experiments. Average S.E. for ATP: 0.18 mM in (A), 0.28 mM in (B); for membrane potential, 16–17 mV. Solid curves drawn by eye, dotted curves (A only) drawn according to Eqns. 1 and 2 (see text).

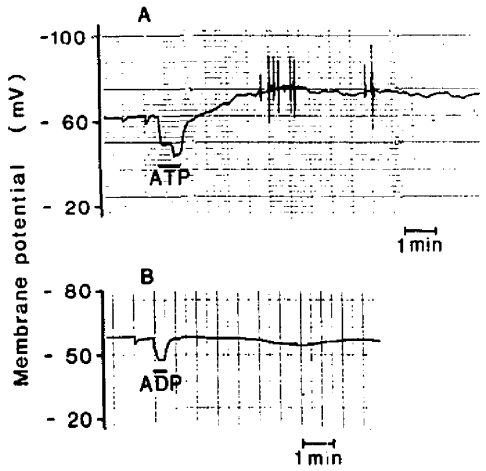

Fig. 4. Membrane hyperpolarization caused specifically by intracellular injection of ATP. Horizontal thick bars indicate the injection interval for ATP (A), or ADP (B) used as a control (separate plasmodium). Sharp depolarizing spike 20–40 s before injection is an artifact due to penetration of the injection pipette. Injection solutions (see Materials and Methods): 500 mM ATP or ADP. Final added cytoplasmic concentrations: approx. 0.5 mM. Note that only ATP, not ADP, induced the gradual hyperpolarization of approx. 12 mV.

minima were reached, both $[ATP]_i$ and membrane potential rebounded slightly. It is likely that such partial recovery in the sustained presence of cyanide arises from activation of the anaerobic glycolytic pathway in *Physarum*, as a response to respiratory blockade [26]. One millimolar NaN_3, also, brought about an ATP depletion nearly parallel to the membrane depolarization during the onset of its inhibition.

With DES by contrast, $[ATP]_i$ barely changed from the control value over the entire period required for maximal depolarization. In Fig. 3B, 5 min after addition of 5 μM DES, the membrane potential had fallen to approx. 30% of the control value, but $[ATP]_i$ was still at approx. 85%. By acting directly on a membrane transport system, DES should not affect cytoplasmic metabolite concentration, except secondarily. Therefore, its observed slow and incomplete depletion of $[ATP]_i$ supports both the accepted idea of DES's mode of action and the postulated existence of an ATP-driven ion pump in *Physarum* membranes.

Further supporting evidence that the major electric generator is an ATPase was obtained by measuring changes of membrane potential after direct injection of nucleotides into microplasmodia. As shown in Fig. 4A, injection of a droplet of ATP solution (to an added concentration of about 0.5 mM) had a complicated effect on the recorded membrane potential. The potential fell about 15 mV during the pipette insertion and liquid injection, but then began recovering to achieve approx. 12 mV hyperpolarization 3–4 min later. Control injections of saline solution, lacking ATP and/or containing ADP, proved the initial depolarization to be an artifact. The effect of ADP injection is shown in Fig. 4B. Transient depolarization still occurred albeit to a smaller extent than in Fig. 4A, but recovery reached only to the control membrane potential and was followed by a slow and slight secondary depolarization. The effect of GTP injection was similar to that of ADP.

Quantitative relations between ATP and membrane potential

Inspection of Fig. 3A reveals that, in response to addition of 10 mM KCN, the initial changes in both $[ATP]_i$ and membrane potential were slow, with the maximal rates of decay delayed 20–30 s after the onset of cyanide entry. For quantitative analysis, the data (out to 1 min) in Fig. 3A have been replotted on semilogarithmic coordinates in Fig. 5A and B, and the linear portions have been fitted by a least-squares method to straight lines. By this maneuver, the second phase of $[ATP]_i$ decay could be described by a single exponential equation:

$$[ATP]_i = A_1 + A_2 e^{-kt} = 0.42 + 1.78\, e^{-0.063t} \text{ (in mM)} \quad (1)$$

in which k is the rate constant in s^{-1}, A_1 is an ATP pool uninfluenced by cyanide, and A_2 is the cyanide-sensitive pool. The analogous equation for the second phase of voltage decay is:

$$V_m = -30 - 139\, e^{-0.064t} \text{ (in mV)} \quad (2)$$

The decay rate constants in these two cases were obtained independently, and their near identity, as well as the demonstration in Fig. 5A and B, emphasizes that after the initial lag period, membrane potential declined in close parallel with $[ATP]_i$.

During the initial period, however, ATP fell more rapidly than membrane potential, and a plot of the potential versus $[ATP]_i$, from points along the smoothed curves, is given in Fig. 5C. As was previously noted by Slayman et al. [27] for *Neurospora*, this plot resembles a Michaelis function, with a small offset voltage added at zero ATP. The plot can be fitted to the sum of a constant term and a rectangular hyperbola (Eqn. 3):

$$V_m = V_o + \frac{V_{pm}[ATP]_i}{K_m + [ATP]_i} = -4 + \frac{-120\,[ATP]_i}{1.1 + [ATP]_i} \quad (3)$$

in which V_o represents the membrane potential in the absence of electrogenic pumping (corresponding to the leak, or ion diffusion component), V_{pm} represents the apparent maximal voltage developed by the pump, and K_m is the ATP concentration which yields half the maximal pump voltage.

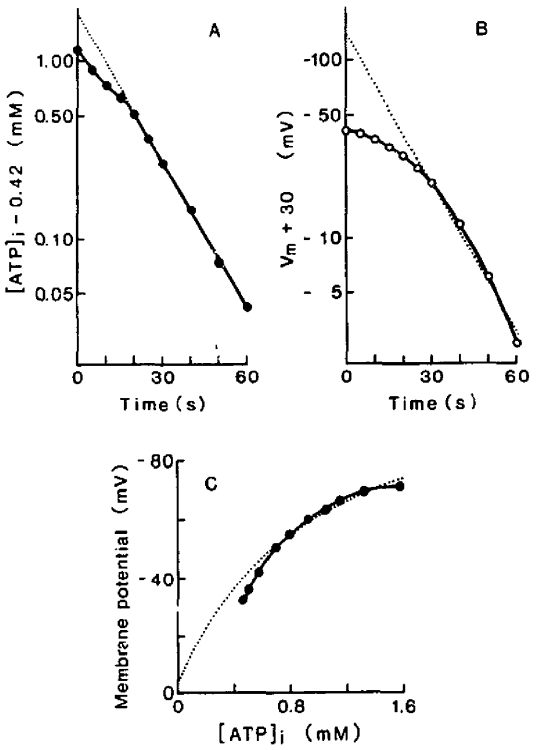

Fig. 5. Kinetic analysis of ATP decay and membrane depolarization during cyanide inhibition. Time-course of ATP decay (A) and membrane depolarization (B) plotted semilogarithmically against time. Data taken from Fig. 3. Solid curves drawn by eye, and dotted lines by least-squares fitting to a single declining exponential function (text Eqns. 1 and 2). Fitted values give: $[ATP]_i - 0.42 = 1.78\ e^{-0.063t}$ (A) and $V_m + 30 = -139\ e^{-0.064t}$ (B). Plot (C) displays membrane potential as a function of $[ATP]_i$, for corresponding time points in (A) and (B). Solid curve drawn by eye. Dotted curve is a Michaelis function plus an added constant (text Eqn. 3), fitted by least squares. Values are: $V_m = -4 - 120\,[ATP]_i/(1.1 + [ATP]_i)$.

The fitted parameter values, shown at the end of Eqn. 3, provide useful comparisons both with the injection experiments described above, and with other published results. The normal steady-state $[ATP]_i$ in *Physarum* is 1.14 ± 0.34 (25) mM, and the injection increment in Fig. 4A was 0.5 mM, so that Eqn. 3 yields an expected ATP-induced hyperpolarization of 11 mV, exactly within the observed range of 11–13 mV. The Michaelis constant, $K_m = 1.1$ mM, itself is in the mid-range of values obtained for plasma membrane ATPases in the true fungi which have been most studied. Slayman et al. [27], using the same technique as here, found $K_m = 2.1$ mM ATP for the proton pump in *Neurospora* plasma membrane, and a value of about 1.3 mM was obtained from ATPase activity in broken membranes of the same organism [28]. Chemical assays of phosphate hydrolysis have also given K_m values between 0.5 mM and 1.5 mM ATP for the plasma membrane ATPases of the yeasts *Saccharomyces* [29] and *Schizosaccharomyces* [30]. The leak voltage, $V_o = -4$ mV, will be considered further in the last section of Results, and the apparent maximal pump voltage, $V_{pm} = -120$ mV, which is physically a composite parameter, will be treated in the Discussion.

Inhibitor effects on net proton flux

Direct evidence identifying protons as the ions electrogenically pumped, to generate the *Physarum* membrane potential, was sought from the comparison of inhibitor effects on net proton flux with that on membrane potential. As shown in Fig. 6A, microplasmodia which were incubated in oxygenated, diluted Pipes buffer displayed a constant, brisk, acid secretion (downward slope of the baseline). Addition of 10 mM neutralized KCN into the suspension resulted, after the large displacement artifact (upstroke in Fig. 6A), in apparent net acid uptake. In these experiments, a significant background alkaline drift was observed, and was quantified by parallel control measurements in the absence of plasmodia (Fig. 6B). After correction for this drift and for the displacement artifact, net proton flux could be calculated from the resultant slopes of pH-versus-time curves. Three independent experiments like that in Fig. 6A gave the average plot of proton flux shown in Fig. 6C (filled circles). The steady-state net proton efflux, amounting to 14 $pmol \cdot s^{-1} \cdot mg^{-1}$ of plasmodium, had decreased to zero within 30 s after cyanide addition, and continued to decrease until about 80 seconds, when it reached a minimum (apparent influx maximum) near -28 $pmol \cdot s^{-1} \cdot mg^{-1}$. This H^+ minimum coincided in time with the minimum of membrane potential (Fig. 6C, open circles). These results are qualitatively consistent with the idea that the electrogenic ion pump in *Physarum* plasma membranes is a proton pump.

Obviously, however, no simple quantitative relationship exists between net proton flux and the membrane potential. The two plotted curves differ in several respects: (a) The rate constant for decrement of flux was only 0.033 s^{-1}, about 50% of that (0.064 s^{-1}) for the exponential phase of voltage decay (see Fig. 5A). (b) During the spontaneous recovery in sustained cyanide (beyond 80 s in Fig. 6C), proton flux rose more quickly than membrane potential, and finally, (c) the direction of net proton flux could be reversed, whereas full inhibition of a pump should only drop the pump flux to zero. Direct pump blockade by DES, also, showed a conversion of net proton flux from the steady-state efflux of approx. 14 $pmol \cdot s^{-1} \cdot mg^{-1}$ to an influx of approx. 8 $pmol \cdot s^{-1} \cdot mg^{-1}$ within 5 min, although a little irregular progress.

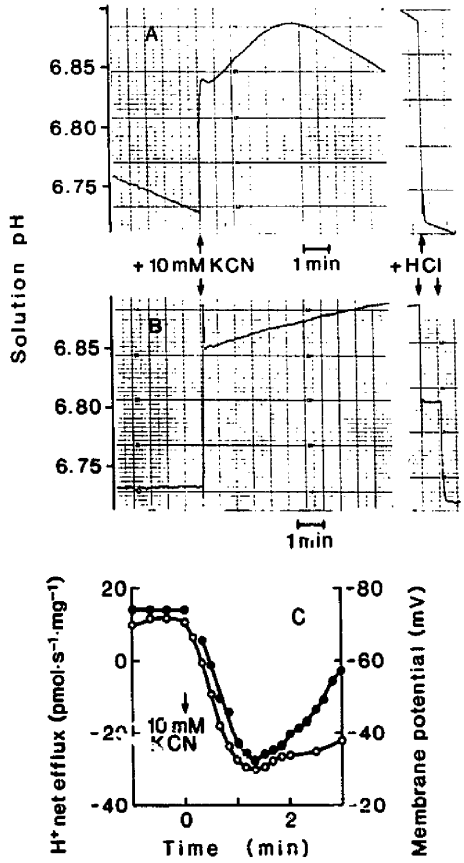

Fig. 6. Change of net proton flux caused by cyanide. Traces show solution pH in 20 ml suspension containing 122 mg dry weight microplasmodia (A) and in the same volume of plasmodia-free dilute Pipes buffer (B) used to control for pH artifacts due to mixing and the alkaline drift. KCN (10 mM) added at the arrows. Abrupt transition and spikes in both traces are mixing artifacts caused by a little pH difference between the suspension or buffer and the added KCN solution, and the transient heterogeneity before complete mixing of KCN with the suspension or buffer. Twenty seconds after the KCN addition, therefore, were not analyzed. Calibration bars generated by adding 10 mM HCl to 85 μM in (A) and to total 90 μM in (B). Proton flux was calculated at 10-s intervals, from the slope (versus time) of the difference curve: Trace (A) minus trace (B). (C) Comparison of net proton flux with membrane potential during cyanide blockade. Plotted points of net proton flux (●) are averages for three experiments, with average S.E. = 0.16 pmol·s^{-1}·mg^{-1} before the KCN addition and 5.26 pmol·s^{-1}·mg^{-1} after that. Membrane potentials (○) replotted from Fig. 3A. Solid curves drawn by eye.

Some passive characteristics of Physarum membranes

These quantitative disparities between proton flux and membrane potential can be accounted for in principle, without disrupting the notion of ATP-dependent proton pumping, if proton permeability is also an important feature of background, passive permeability of *Physarum* membranes.

In order to examine this possibility, the pH sensitivity of membrane potential was determined during metabolic blockade by cyanide, where pump voltage should be reduced to 30–40% of its control value (see Figs. 1A and 3A), thus accentuating the relative contributions of passive processes to membrane electrical characteristics. Minimal membrane potential was measured as a function of varied external pH, pH_o (Fig. 7A). Results show essentially a monotonic decline of membrane potential with falling pH_o between pH 6.0 and pH 4.7 (the least-squares slope of 26 mV/pH), but a smaller slope than that of the equilibrium diffusion potential for H^+ (E_H). This result indicates a significant, but not predominant, permeability of the membrane for protons.

Ions other than H^+ to which the *Physarum* membrane might be significantly permeable include Ca^{2+}, Na^+, Cl^-, and K^+. The first three, however, could be ruled out relatively easily as major contributors to the diffusion potential inferred from voltage-versus-ATP data (Fig. 5, Eqn. 3). Calcium ions, present at a free cytosolic concentration of 300 nM or less [31] and a normal extracellular concentration of 1 mM (see Table I), have a diffusion potential of about +110 mV, far positive to any value ever observed for *Physarum* membrane potential. Likewise, changes of extracellular Na^+ and Cl^- had little effect on the resting potential of microplasmodia: raising $[Na^+]_o$ from 3 to 30 mM at fixed $[Cl^-]_o$ depolarized only 6–7 mV, and similarly raising $[Cl^-]_o$ by substituting methanesulfonate for

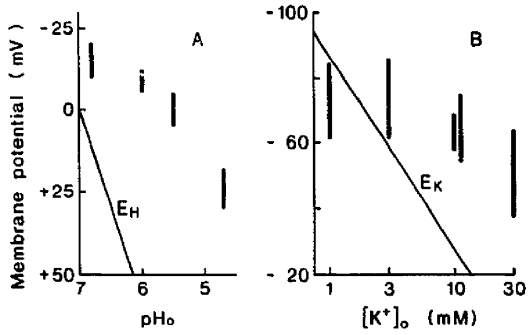

Fig. 7. pH effect on the membrane potential of cyanide-inhibited microplasmodia (A) and effect of $[K^+]_o$ on the membrane potential of uninhibited microplasmodia (B). Plasmodia were equilibrated at each test pH for 10–20 min (A), or in standard Pipes buffer for at least 10 min (B). After the recorded potential had stabilized, 10 mM KCN-containing pH-medium (Table I) (A) or one of the special K-media (Table I) (B) was applied. Values were read at the minimal voltage in (A) and at a new steady level of potential (usually 2–3 min after) in (B). The diagonal straight lines designate the equilibrium diffusion potentials for H^+ (E_H) (A) and K^+ (E_K) (B), assuming $[H^+]_c = 10^{-7}$ M and $[K^+]_c = 29.4$ mM. Each vertical bar represents the range of membrane potentials recorded from three separate experiments in (A) and seven separate experiments in (B).

chloride from 2 to 30 mM hyperpolarized by only 3 mV.

Considerably larger effects of changing extracellular concentration were observed with K^+. Fig. 7B shows a plot of membrane potential against extracellular K^+ concentration, $[K^+]_o$. For $[K^+]_o$ of 3 mM and above, the least-squares slope was 21 mV/log unit. Thus, the effective permeability, which is strictly the product of permeability and concentration, for K^+ is similar to that for H^+ in plasmodial membranes of *Physarum*.

These results resemble those obtained on droplet membranes from caffeine-treated *Physarum* [1], in that passive permeability of *Physarum* membranes is controlled by H^+, and secondarily by K^+. In the present experiments, however, the relative effective permeabilities for H^+ and K^+ proved closer together than was true for the droplet membranes. Knowledge of passive permeabilities enables us to calculate the expected passive component of membrane potential. At $pH_o = 6.8$ in standard Pipes buffer, the effective permeabilities for K^+ and H^+ are roughly equivalent, and the passive component of membrane potential can be estimated as the average of individual diffusion potentials for K^+ (E_K) and H^+ (E_H). $[K^+]_o$ is 11.4 mM, and cytosolic K^+ concentration, $[K^+]_c$, is 29.4 mM [1]. Cytosolic pH, pH_c, is assumed to be about 7.0 [32,33]. The Nernst equation then yields $E_K = -24$ mV, and $E_H = +12$ mV, so the expected passive component of membrane potential would be -6 mV, tolerably close to the value of -4 mV obtained in Fig. 5C.

Questions of how the apparent maximal pump voltage (-120 mV) and the peculiarities of net proton flux revealed in Fig. 6C fit into the combined picture of K^+ and H^+ diffusion and electrogenic H^+ pumping will be considered in the Discussion.

Discussion

Two previous studies have been carried out on the electrical characteristics of plasma membranes in the slime mold *Physarum polycephalum*. The first [1] used a model preparation, caffeine-induced cytoplasmic droplets, to examine the effects of metabolic inhibitors and extracellular ions. The dominant features of that membrane proved to be passive proton permeability and active electrogenic ion pumping, with indirect evidence identifying the pump ions as protons. The second study [34] succeeded in direct electrical recording from microplasmodia, and developed a quantitative description of the ion pump from the electrical response of plasmodia to pH_o changes.

The present experiments, also on microplasmodia rather than droplets, sought direct evidence about whether the pump in fact transports protons and is fueled by ATP; that is, whether the electrogenic pump in *Physarum* membranes is an H^+-ATPase and is of the same enzyme class as the well-known plasma membrane proton pumps of the true fungi such as *Neurospora*, *Saccharomyces*, and *Schizosaccharomyces* [30].

Major conclusions

ATP fueling of the pump is clearly demonstrated by the data in Figs. 3, 4 and 5: (a) membrane potential falls almost in parallel with ATP concentration during the onset of metabolic inhibition; (b) the deviation implied in (a) can be described quantitatively by a Michaelis-Menten relationship between pump electron motive force and $[ATP]_i$, which yields a Michaelis constant of 1.1 mM ATP, closely similar to that for other fungal proton pumps; and (c) microinjection of ATP into microplasmodia yields hyperpolarization which is quantitatively consistent with (b).

Specific pumping of protons is qualitatively supported by the behavior of net proton flux during metabolic inhibition (Fig. 6) and during direct pump blockade by DES. However, the fact that net proton flux is actually inward (not simply zero) during maximal respiratory blockade, clearly indicates that more factors than simply a proton pump contribute to proton movements through *Physarum* membranes. The nature of relevant additional factors remains to be determined, but some estimate of their magnitude can be obtained as follows.

In the complete membrane circuit, all current driven outward by the pump must return through passive mechanisms, and the net proton flux will be only the difference between pumped efflux and all equivalent proton re-entry processes. We [1] calculated membrane resistivity of uninhibited *Physarum* droplets to be 13–40 $k\Omega \cdot cm^2$ from the voltage displacement produced by injection of rectangular pulses of inward current, and the surface area of the droplet calculated from the measured diameter, assuming spherical geometry. Fingerle and Gradmann [34], also, using a linear equivalent circuit, calculated the leak resistance of the pump in microplasmoidal membranes to be 3 and 13 $k\Omega \cdot cm^2$. Here, we assume the leak resistance in microplasmodial membranes to be 20 $k\Omega \cdot cm^2$, which demands a current of 3.5 $\mu A/cm^2$ (for zero leakage potential, instead of -4 mV) to produce the normal resting potential of -70 mV and 6.0 $\mu A/cm^2$ to produce the maximal pump voltage ($V_{pm} = -120$ mV). These correspond to the chemical flux of 35 and 60 $pmol \cdot cm^{-2} \cdot s^{-1}$. If assumed 1 mg dry weight plasmodia to have 2.9 ± 0.4 μl cell volume, and microplasmodia in our culture to be spheres of 200–500 μm diameter lacking the membrane invaginations, the actual measured steady-state net efflux of 14 $pmol \cdot s^{-1} \cdot mg^{-1}$ corresponds to 20–40 $pmol \cdot cm^{-2} \cdot s^{-1}$. Thus, considerable fraction of the total pump current appears as the net efflux.

Comparison with other systems

Membrane parameters computed in Eqn. 3 are: (i) net ion diffusion potential, $V_o = -4$ mV; (ii) apparent maximal pump voltage, $V_{pm} = -120$ mV; and (iii) the Michaelis constant, $K_m = 1.1$ mM ATP. We have already mentioned (see Results) that K_m is in the mid-range of values observed by several investigators for fungal H^+-ATPases. It is very high, however, compared with K_m values (10–30 μM) commonly observed in algae [8] or for any of the plasma membrane cation ATPases in animal cells (see Ref. 30). Neither the chemical basis for this difference, nor its physiological significance, is yet apparent.

The major reaction product of most of the plasma-membrane ATPases is electric current, and the apparent maximal pump voltage is simply the product of that current and the appropriate leakage resistance of the membrane. Its value of -120 mV is less than 40% of the value obtained in *Neurospora* (-311 mV) [27]. This difference probably arises entirely from lower current densities (e.g., 3.5 or 6.0 $\mu A/cm^2$) in the *Physarum* membrane, as compared with that in the *Neurospora* membrane (e.g., 20 $\mu A/cm^2$) [27]. An interesting additional point, however, is that the actual stalling potentials for the two proton pumps probably also differ by about a factor of two, since the stoichiometry of charge transport/ATP hydrolysis is 1 in *Neurospora* [30] and probably 2 in *Physarum* [34].

The net ion diffusion potential (-4 mV) is rather small compared with those estimated in most other fungi and in plants. The values obtained by similar analysis in *Neurospora* ranged between -7 and -50 mV, depending upon the ambient temperature and other conditions for ATP and voltage measurements [27]. In the yeast *Saccharomyces* indirect estimates of residual membrane potential in energy-deprived cells have given values of -20 to -40 mV [35]. And in *Acetabularia* [36], Characean algea [37] and higher plants [38], cell membranes in the 'pump-off' state all have membrane potentials near the potassium equilibrium potential, e.g., about -80 mV. The evident difference between these other organisms and CN^--inhibited *Physarum* plasmodia is that the latter discriminate rather poorly between two ion species, K^+ and H^+, which have opposing equilibria of about the same magnitude. Whether this lack of discrimination is a natural physiological state of the *Physarum* membrane or reflects secondary and/or non-specific effects of the inhibitors is unresolved.

A next step to elucidate the passive characteristics of *Physarum* membranes and the reaction mechanisms of the pump including stoichiometry of *Physarum* pump between proton extrusion and ATP hydrolysis might be current-voltage analysis of the membrane of internally perfused plasmodia by voltage-clamp methods.

Acknowledgements

This work was supported by research grants from the Ministry of Education of Japan. We thank Dr. S. Kawano for providing microplasmodia of *Physarum polycephalum*, Dr. H. Miyamoto for his generous permission to use his facilities and for his helpful discussion, Dr. H. Kitasato for his helpful discussion, and Dr. C.L. Slayman for his valuable and critical discussion and for his critical reading of the manuscript.

References

1 Kuroda, H. and Kuroda, R. (1981) J. Gen. Physiol. 78, 637–655.
2 Slayman, C.L. (1965) J. Gen. Physiol. 49, 69–92.
3 Slayman, C.L. (1965) J. Gen. Physiol. 49, 93–116.
4 Serrano, R. (1980) Eur. J. Biochem. 105, 419–424.
5 Kitasato, H. (1968) J. Gen. Physiol. 52, 60–87.
6 Spanswick, R.M. (1972) Biochim. Biophys. Acta 288, 73–89.
7 Shimmen, T. and Tazawa, M. (1977) J. Membr. Biol. 37, 167–192.
8 Mimura, T., Shimmen, T. and Tazawa, M. (1983) Planta 157, 97–104.
9 Mercier, A.J. and Poole, R.J. (1980) J. Membr. Biol. 55, 165–174.
10 Doll, S. and Hauer, R. (1981) Planta 152, 153–158.
11 Daniel, J.W. and Rusch, H.P. (1961) J. Gen. Microbiol. 25, 47–59.
12 Camp, W.G. (1936) Bull. Torrey Club 63, 205–210.
13 Miyamoto, H., Ikehara, T., Sakai, T. and Yamaguchi, H. (1976) Acta Med. Kinki Univ. 1, 75–85.
14 Yoshimoto, Y., Sakai, T. and Kamiya, N. (1981) Protoplasma 109, 159–168.
15 Hiramoto, Y. (1962) Exp. Cell Res. 27, 416–426.
16 Umrath, K. (1932) Protoplasma 16, 173–188.
17 Walker, N.A. (1955) Austr. J. Biol. Sci. 8, 477–489.
18 Lowry, O.H., Rosebrough, N.J., Farr, A.L. and Randall, R.J. (1951) J. Biol. Chem., 193, 265–275.
19 Winkler, H.H. and Wilson, T.H. (1966) J. Biol. Chem. 241, 2200–2211.
20 Balke, N.E. and Hodges, T.K. (1977) Plant Sci. Lett. 10, 319–325.
21 Bowman, B.J., Mainzer, S.E., Allen, K.E. and Slayman, C.W. (1978) Biochim. Biophys. Acta 512, 13–28.
22 Kuroda, H., Warncke, J., Sanders, D., Hansen, U.-P., Allen, K.E. and Bowman, B.J. (1980) in Plant Membrane Transport: Current Conceptual Issues (Spanswick, R.M., Lucas, W.J. and Dainty, J., eds.), pp. 507–508, Elsevier/North-Holland, Amsterdam.
23 Lowendorf, H.S., Bazinet, G.F., Jr. and Slayman, C.W. (1975) Biochim. Biophys. Acta 389, 541–549.
24 Bowman, B.J. and Slayman, C.W. (1979) J. Biol. Chem. 254, 2928–2934.
25 Blatt, M.R., Rodriguez-Navarro, A. and Slayman, C.L. (1987) J. Membr. Biol. 98, 169–189.
26 Ohta, J. (1954) J. Biochem. 41, 489–497.
27 Slayman, C.L., Long, W.S. and Lu, C.Y.-H. (1973) J. Membr. Biol. 14, 305–338.
28 Bowman, B.J. and Slayman, C.W. (1977) J. Biol. Chem. 252, 3357–3363.
29 Borst-Pauwels, G.W.F.H. and Peters, P.H.J. (1981) Biochim. Biophys. Acta 642, 173–181.
30 Goffeau, A. ad Slayman, C.W. (1981) Biochim. Biophys. Acta 639, 197–223.
31 Kuroda, R., Hatano, S., Hiramoto, Y. and Kuroda, H. (1988) in Cell Dynamics (Tazawa, M., ed.), Protoplasma Suppl. 1, pp. 72–80.

32 Morisawa, M. and Steinhardt, R.A. (1982) Exp. Cell Res. 140, 341–351.
33 Kohama, K., Tanokura, M. and Yamada, K. (1984) FEBS Lett. 176, 161–165.
34 Fingerle, J. and Gradmann, D. (1982) J. Membr. Biol. 68, 67–77.
35 Ballarin-Denti, A., Den Hollander, J.A., Sanders, D., Slayman, C.W. and Slayman, C.L. (1983) Biochim. Biophys. Acta 778, 1–16.
36 Gradmann, D. (1975) J. Membr. Biol. 25, 183–208.
37 Walker, N.A. (1980) in Plant Membrane Transport: Current Conceptual Issues (Spanswick, R.M., Lucas, W.J. and Dainty, J., eds.), pp. 287–300, Elsevier/North-holland, Amsterdam.
38 Higinbotham, N. (1973) Annu. Rev. Plant Physiol. 24, 25–46.